CONTROL OF BURSTING SYNCHRONIZATION IN NETWORKS OF THERMALLY SENSITIVE NEURONS WITH CHEMICAL SYNAPSES

Carlos A. S. Batista
Department of Physics
Federal University of Parana
Brazil
batiscarlos@gmail.com

Ricardo L. Viana
Department of Physics
Federal University of Parana
Brazil
viana@fisica.ufpr.br

Abstract

Thermally sensitive neurons present bursting activity for certain temperature ranges, characterized by fast repetitive spiking of action potential followed by a short quiescent period. Synchronization of bursting activity is possible in networks of coupled neurons, and it is sometimes an undesirable feature. Control procedures can suppress totally or partially this collective behavior, with potential applications in deep brain stimulation techniques. We investigate the control of bursting synchronization in small-world networks of Hodgkin-Huxley type thermally sensitive neurons with chemical synapses through two different strategies. One is the application of an external time-periodic electrical signal and another consists of a time-delayed feedback signal. We consider the effectiveness of both strategies in terms of protocols of applications suitable to be applied by pacemakers.

Key words

neural networks, synchronization, bursting, control

1 Introduction

A dynamical description of a bursting neuron requires the use of mathematical models possessing two timescales: (i) a fast time scale characterized by repetitive spiking; and (ii) a slow timescale with bursting activity, where neuron activity alternates between a quiescent state and spiking trains. The spiking dynamics of the action potentials can be described by the Hodgkin-Huxley model, which is a conductance-based model of an excitable neuron, its protein molecule ion channels (Na^+ and K^+) being represented by conductances and its lipid bilayer by a capacitor. Bursting activity in Hodgkin-Huxley models of neuronal activity is usually included through additional Calcium currents.

Bursting activity can be also observed in thermally sensitive neurons: a Hodgkin-Huxley type model of thermally sensitive neurons has been proposed by Huber and Braun [Braun *et al.* 1998, 1999, 2000, 2001], which describes spike train patterns experimentally observed in facial cold receptors and hypothalamic neurons of the rat [Braun *et al.*, 1999], electro-receptors organs of freshwater catfish [Schäfer *et al.*, 1995], and caudal photo-receptor of the crayfish [Feudel *et al.*, 2000].

2 The model

A computational model of a neural network consists on a network architecture, which specifies how neurons are connected, and a neuronal dynamics attached to each unit, or node. The connections among neurons (of electrical or chemical nature) are the links of this network.

2.1 Neuronal dynamics

The main dynamical variable for the ith neuron, belonging to a given network with $i = 1, 2, \ldots N$, is the membrane potential V_i, whose time evolution is influenced by a number of currents from different sources, in the form (the membrane potential is measured in mV and time in ms):

$$C_M \frac{dV_i}{dt} = -I_{iNa} - I_{iK} - I_{isd} - I_{isa} - I_{i\ell}, \quad (1)$$

where C_M is the membrane capacitance. I_{iNa}, I_{iK}, and $I_{i\ell}$ are, respectively, the Na^+ and K^+ ionic currents and the leak current, like in the Hodgkin-Huxley model (currents, or rather, current densities, are measured in $\mu A/cm^2$). The currents I_{isd} and I_{isa} refer to intrinsic sub-threshold oscillations: I_{isd} to the intrinsic membrane depolarization current, and I_{isa} to the repolarization oscillations. We associate a given conductance (measured in mS/cm^2) to each current, in the

following form

$$I_{iNa} = \rho g_{Na} a_{Na}(V_i - V_{Na}), \quad (2)$$

$$I_{iK} = \rho g_K a_K(V_i - V_K), \quad (3)$$

$$I_{isd} = \rho g_{sd} a_{sd}(V_i - V_{sd}), \quad (4)$$

$$I_{isa} = \rho g_{sa} a_{sa}(V_i - V_{sa}), \quad (5)$$

$$I_{i\ell} = g_\ell(V_i - V_\ell), \quad (6)$$

where g_{Na}, g_K, g_{sd}, g_{sa}, g_ℓ are the maximal conductances, and the reversal (Nernst) potentials for each ionic current are denoted by V_{Na}, V_K, V_{sd}, and V_{sa}.

It turns out that I_{Na} and I_K are simplified fast Hodgkin-Huxley currents representing Na^+ and K^+ channels, respectively. These fast currents are responsible for spike generation [6]. I_{sd} and I_{sa} are slow currents which are responsible for subthreshold activation, i.e., they activate more slowly at lower membrane potentials. These slow currents are necessary to generate bursting behavior.

We would like to remark that I_{sd} represents a generic voltage-gated Ca^{2+} channel and I_{sa} a current with behavior reminiscent of SK-channels. However, while real SK-channels are Ca^{2+}-sensitive rather than voltage-sensitive, the combination of I_{sa} and I_{sd} present in this model yields a behavior similar to voltage-gated Ca^{2+} channels coupled with SK-channels. This procedure of replacing a ion-sensitive to a voltage-gated channel is common in biophysical models of neurons: for example the inactivation of fast Na^+ channels is not really voltage-gated, but it is modeled this way in many models of neuronal dynamics. Hence this model represents SK channels as voltage-sensitive, as I_{sa} reasonably behaves like SK without the need for keeping track of intracellular Ca^{2+}.

For thermally sensitive neurons ρ is a scale factor depending on the temperature T which, for the kinetic ion model, is $\rho = \rho_0^{\frac{(T-T_0)}{\tau_0}}$, where ρ_0, T_0 and τ_0 are parameters.

The activation currents a_{Na}, a_K, a_{sd}, and a_{sa} have their evolution described by the following differential equations

$$\frac{da_{Na}}{dt} = \frac{\phi}{\tau_{Na}}(a_{Na,\infty} - a_{Na}), \quad (7)$$

$$\frac{da_K}{dt} = \frac{\phi}{\tau_K}(a_{K,\infty} - a_K), \quad (8)$$

$$\frac{da_{sd}}{dt} = \frac{\phi}{\tau_{sd}}(a_{sd,\infty} - a_{sd}), \quad (9)$$

$$\frac{da_{sa}}{dt} = \frac{\phi}{\tau_{sa}}(-\eta I_{isd} - \gamma a_{sa}), \quad (10)$$

where τ_{Na}, τ_K, τ_{sd} and τ_{sa} are characteristic times and η and γ other parameters, and we define a second temperature-dependent scale factor $\phi = \phi_0^{\frac{(T-T_0)}{\tau_0}}$. Any inactivation of the ionic channels are neglected [1]. The

factor η serves for increasing Ca^{2+} concentration following I_{sa}, and γ accounts for active elimination of intracellular Ca^{2+}.

The activation functions in the stable state, namely $a_{Na,\infty}$, $a_{K,\infty}$, $a_{sd,\infty}$, are related to the membrane potential by sigmoid functions:

$$a_{Na,\infty} = \frac{1}{1 + \exp[-s_{Na}(V_i - V_{0Na})]}, \quad (11)$$

$$a_{K,\infty} = \frac{1}{1 + \exp[-s_K(V_i - V_{0K})]}, \quad (12)$$

$$a_{sd,\infty} = \frac{1}{1 + \exp[-s_{sd}(V_i - V_{0sd})]}, \quad (13)$$

where s_{Na}, s_K, and s_{sd} are constants and V_{0Na}, V_{0K}, and V_{0sd} are activation voltages. The parameter values to be used in this paper are found in [Batista et al., 2013]. The temperature we use in numerical simulations is $T = 8.0^o C$, for which we find bursting behavior characterized by repetitive spiking for which the interspike interval (ISI) exhibits a chaotic evolution, followed by a quiescent regime.

2.2 Synaptic coupling

It is known that, in real neural networks, neurons are neither completely nor randomly connected. Studies of connectivity of some neural networks in both the microscopic (C. elegans) and mesoscopic (cat cortico-cortical matrix) suggest that the networks exhibit the so-called small-world (SW) property, since they display features of both regular and random lattices.

Here we will consider a small-world network, consisting of a lattice in which each neuron has both local and nonlocal connections. A neuron is connected to its nearest and next-to-nearest neighbors, as well as with a small number of randomly chosen non-local neurons. It can be shown that the resulting network has a small average pathlength, in the same way as random networks do, but still retaining an appreciable degree of clustering, as in regular lattices.

The coupling among neurons enters in the model through a synaptic current I_{syn} which is added in the differential equation (1) governing the behavior of the membrane potential for the ith neuron:

$$C_M \frac{dV_i}{dt} = -I_{iNa} - I_{iK} - I_{isd} - I_{isa} - I_{i\ell} + I_{syn}, \quad (14)$$

where

$$I_{syn} = g_c \sum_{j=1}^{N} a_{ij} r_j(t)(V_{syn} - V_j), \quad (15)$$

with g_c as a coupling strength with conductance dimensions, a_{ij} are the elements of the adjacency matrix corresponding to a small-world network, V_{syn} is the
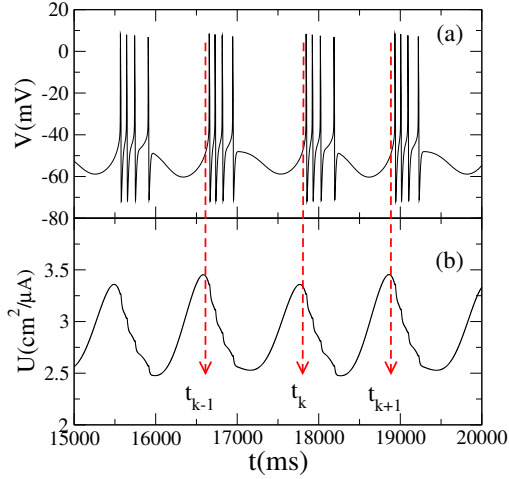
Figure 1. Time evolution of the (a) membrane potential (b) recovery variable (inverse of the sub-threshold repolarization current) for an isolated neuron at temperature $T = 8.0^0C$. The arrows indicate the times at which bursting cycles begin.

synaptic reverse potential, and $r_j(t)$ is the fraction of bond receptors of the jth neuron, whose time-evolution is described by

$$\frac{dr_j}{dt} = \left(\frac{1}{\tau_r} - \frac{1}{\tau_d}\right) \frac{1 - r_j}{1 + \exp(-V_j + V_0)} - \frac{r_j}{\tau_d}, \quad (16)$$

where V_j is the membrane potential of the post-synaptic neuron, τ_r and τ_d are characteristic rise and decay times, respectively, of the chemical synapse. The numerical values of the coupling parameters to be used in the simulations reported in this work can be found in [Batista *et al.*, 2013].

3 Bursting synchronization

A representative example of bursting is shown in Fig. 1(a): the membrane potential of a single neuron described by the Huber-Braun model undergoes repetitive spiking after periods of quiescent behavior. The beginning of each outburst of repetitive spiking is also a local maximum of the recovery variable $U = 1/a_{sa}$, and may be considered as the beginning of a bursting cycle [Fig. 1(b)]. This makes possible to define a geometric phase. Let t_k the time at which a kth bursting cycle begins. The phase is obtained by simple interpolation as

$$\varphi(t) = 2\pi k + 2\pi \frac{t - t_k}{t_{k+1} - t_k}, \qquad (t_k < t < t_{k+1}), \quad (17)$$

and increases monotonically with time.

In the numerical simulations of SW networks of thermally sensitive neurons we shall use networks with

$N = 2000$, with shortcut probability $p = 0.01$ and coupling strength $g_c = 0.01 mS/cm^2$, unless stated differently. Solving the coupled system of $5N$ equations (using a fourth-order Runge-Kutta method with fixed stepsize) yields $V_i(t)$ for each neuron, such that we can trace its time evolution and the times t_k at which the bursting cycles occur. After a sufficiently long integration we can retrace the time series and compute, using Eq. (17), the time evolution of the corresponding phase.

One of the effects of coupling is to induce phase synchronization of bursting: $\varphi_1(t) = \varphi_2(t) = \ldots \varphi_N(t)$, in such a way that the coupled neurons, even though not fully synchronized, are able to display a collective effect, bursting at the same time. The mean field of a network of synchronized bursters displays large-amplitude oscillations reflecting the coherent behavior of the assembly.

Two useful numerical diagnostics of bursting synchronization are the mean field of the network and the Kuramoto's order parameter. The former is obtained by averaging the membrane voltages of all neurons belonging to the network at a given time: $V_m = (1/N) \sum_{i=1}^{N} V_i$. If the bursters are non-synchronized, i.e. if they begin their bursting cycles at different times, the corresponding mean field exhibits small-amplitude noisy fluctuations with time. In a synchronized state, however, the mean field time evolution displays large-amplitude oscillations. The expected effect of the control is thus the reduction to minimal levels of the network mean field.

The order parameter is defined as

$$z(t) = R(t) \exp\left(i\Phi(t)\right) \equiv \frac{1}{N} \sum_{j=1}^{N} \exp(i\varphi_j(t)), \quad (18)$$

where R and Φ are the amplitude and angle, respectively, of a centroid phase vector for a one-dimensional lattice with periodic boundary conditions. If the neurons are uncoupled, for example, their bursting phases $\varphi_i(t)$ are expected to be uncorrelated such that their contribution to the result of the summation in Eq. (18) is typically small (due to statistical coincidences). In the limit of an infinite site ($N \to \infty$) we expect $R(t)$ to vanish. On the other hand, in a completely phase synchronized state the order parameter magnitude asymptotes the unity, indicating a coherent superposition of the phase vectors at each time. We usually compute the time averaged order parameter magnitude, which we denote as $\overline{R}$.

The time-averaged order parameter magnitude is plotted, in Fig. 2, against the coupling strength g_c, for small-world networks with shortcut probabilities ranging from zero to 0.02. When the latter parameter is zero, the network has regular connections only, and thus it is unlikely to display synchronized behavior, if the coupling strength is small enough. In fact $\overline{R}$ fluctuates between 0.05 and 0.40 in the coupling parameter
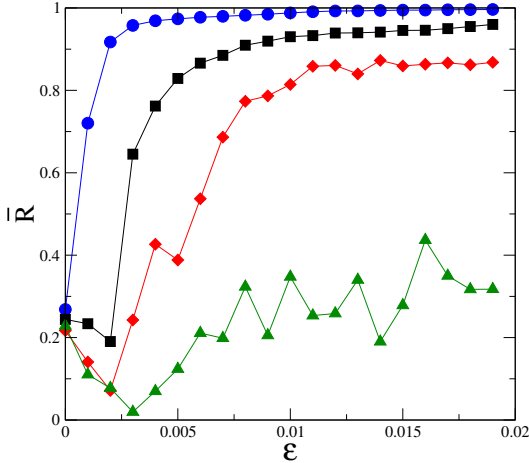
Figure 2. Time-averaged order parameter magnitude as a function of the coupling strength of small-world networks with different values of the shortcut probability p: 0.0001 (green triangles), 0.001 (red lozenges), 0.004 (black squares), 0.020 (blue circles).

Figure 3. Time evolution of the external driving signal I_{ext} [(a) and (b)], mean field [(c) and (d)] and order parameter magnitude [(e) and (f)] for $\omega = 8Hz$, $I_0 = 0.10\mu A/cm^2$ [(a), (c) and (e)] and $0.15\mu A/cm^2$ [(b), (d) and (f)].

range considered [green triangles in Fig. 2].

4   Control of synchronization

Inspired in techniques of deep brain stimulation, in which an external time-periodic electric signal is applied to a cortical area to mitigate abnormal rhythms appearing in pathological conditions, we can investigate the control of bursting synchronization through: (i) a time-periodic signal with a given amplitude and frequency, (ii) a time-delayed feedback signal.

4.1   External time-periodic signal

A time-periodic signal applied to a given neuron can be represented by an external injected current of amplitude I_0 (in $\mu A/cm^2$) and frequency ω (in kHz) of the form $I_{ext} = I_0 \sin(\omega t)$, which is added to the right-hand side of Eq. (1). In strongly coupled networks (like globally or power-law coupled neurons) this intervention can be made on a single selected neuron. For scale-free networks, where there is a strongly connected hub, the latter can be the target of the intervention. In sparsely connected networks, like small-world or random ones, it is unfeasible to randomly select a single neuron, since it is so poorly connected that a modification in its dynamics does not influence the network in a significant way. Hence we choose to make the intervention in all neurons. This is biologically feasible since the electrodes injecting an AC current into a given region of the brain do modify the extracellular field potentials for a number of nearby neurons.

Figures 3(a) and 3(b) depict the time evolution of the external driving signal I_{ext} for $\omega = 8Hz$, $I_0 = 0.10\mu A/cm^2$ and $0.15\mu A/cm^2$, respectively. In the

former case, the effect of the driving signal is weak, and we observe a small reduction in the mean field amplitude [Fig. 3(c)] and likewise a small decrease of the order parameter magnitude [Fig. 3(e)]. Actually the latter undergoes low-frequency oscillations, characterizing a kind of beat. For larger amplitude, however, the mean field oscillation amplitudes decrease [Fig. 3(d)] indicating that the synchronized bursting is partially suppressed in this case. This observation is reinforced by the behavior of the order parameter [Fig. 3(f)], although with the same kind of beat.

4.2   Time-delayed feedback control

According to the value that the mean field takes on for a given time t and its value at an earlier time τ (the control delay) we can design a feedback signal to be applied to the network so as to drive the system out of a synchronized state. This is feasible if a probe is inserted in the network measuring the mean field at different times, and integrating the effect of time-delayed values into a feedback scheme which applies to the network a control signal. The latter is similar in essence to the one studied in the previous section, but its amplitude and frequency are no longer constants but instead determined by the network dynamics itself.

Let $V_m(t)$ and $V_m(t - \tau)$ be the neuronal mean field measured at two times with a delay τ (measured in ms). The feedback electric signal is $I_{feed} = g_f[V_m(t-\tau) - V_m(t)]$, where g_f is a control amplitude (also with conductance dimensions) which may or may not vary during the application, according to the protocol used. The intensity of the control signal is thus proportional to the difference between the actual mean field and the time-delayed one.

The effect of a free-running time-delayed feedback
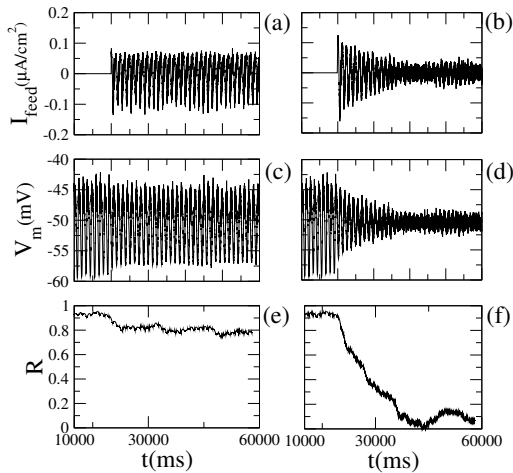
Figure 4. Time evolution of the free-running time-delayed feedback signal I_{feed} [(a) and (b)], mean field [(c) and (d)], and order parameter magnitude [(e) and (f)] for $g_c = 0.01 mS/cm^2$ [(a),(c),(e)] and $0.015 mS/cm^2$ [(b),(d),(f)]. In both cases $\tau = 2ms$

signal is illustrated by Fig. 4, obtained for two different values of g_f and the same values of the time delay $\tau = 2ms$. In Fig. 4(a) and 4(b) we plot the time evolution of the feedback signals I_{feed} for $g_f = 0.010 mS/cm^2$ and $0.015 mS/cm^2$, respectively. We observe that, after the feedback signal is switched on, the oscillations of the mean field V_m are just slightly decreased for $g_f = 0.010 mS/cm^2$ [Fig. 4(c)] and much more diminished for $0.015 mS/cm^2$ [Fig. 4(d)]. Indeed, after the beginning of the control the order parameter magnitude decreases to 0.8 in the former case [Fig. 4(e)] and to almost zero in the latter [Fig. 4(f)].

Acknowledgements

References

H. A. Braun, M. T. Huber, M. Dewald, K. Schäfer, and K. Voigt, Int. J. Bifurcat. Chaos **8**, 881 (1998).

H. A. Braun, M. Dewald, K. Schäfer, K. Voigt, X. Pei, K. Dolan, and F. Moss, J. Comput. Neurosci. **7**, 17 (1999).

W. Braun, B. Eckhardt, H. A. Braun, and M. Huber, Phys. Rev. E **62**, 6352 (2000).

H. A. Braun, M. T. Huber, N. Anthes, K. Voigt, A. Neiman, X. Pei, and F. Moss, Biosystems **62**, 99 (2001).

K. Schäfer, H. A. Braun, R. C. Peters, and F. Bretschneider, Pflügers Arch. - Eur. J. Physiol. **429**, 378 (1995).

U. Feudel, A. Neiman, X. Pei, W. Wojtenek, H. Braun, M. Huber, and F. Moss, Chaos **10**, 231 (2000).